NON-FERMI-LIQUID BEHAVIOR AND MAGNETIC FLUCTUATIONS AT THE QUANTUM PHASE TRANSITION IN $CeCu_{6-x}Au_x$*

H. v. Löhneysen[a,b], C. Pfleiderer[a], A. Schröder[a,c]
AND O. Stockert[a,d]

[a]Physikalisches Institut, Universität Karlsruhe
76128 Karlsruhe, Germany
[b]Institut für Festkörperforschung, Forschungszentrum Karlsruhe
76021 Karlsruhe, Germany
[c]Department of Physics, Kent State University
Kent, Ohio 44242, USA
[d]Max-Planck-Institut für chemische Physik fester Stoffe
01187 Dresden, Germany

$CeCu_{6-x}Au_x$ has become a prototype heavy-fermion system where, starting from not magnetically ordered $CeCu_6$, Au doping introduces long-range incommensurate antiferromagnetism for $x > x_c \approx 0.1$. At the critical concentration x_c, the unusual magnetic fluctuations probed by inelastic neutron scattering lead to non-Fermi-liquid behavior, *i.e.* to anomalous low-temperature thermodynamic and transport properties. In magnetically ordered alloys, hydrostatic pressure can be employed to tune the magnetic–nonmagnetic transition. The effect of pressure in suppressing the antiferromagnetic order is contrasted by the effect of a magnetic field by way of a detailed study for $x = 0.2$.

1. Introduction

In many Heavy-Fermion Systems (HFS), the strength of the conduction-electron$-f$-electron exchange interaction can be tuned by composition or pressure, giving rise to either dominant Kondo or RKKY interactions [1]. This offers the possibility to induce a zero-temperature magnetic–nonmagnetic transition. In the vicinity of this transition Non-Fermi-Liquid (NFL)

---

* Presented at the XII School of Modern Physics on Phase Transitions and Critical Phenomena, Lądek Zdrój, Poland, June 21–24, 2001.

behavior [2] manifests itself as a strong deviation of thermodynamic and transport properties from Fermi-Liquid (FL) predictions. The linear specific-heat coefficient $\gamma = C/T$ acquires an unusual temperature dependence, often $\gamma \sim -\ln(T/T_0)$, and the T-dependent part of the electrical resistivity $\Delta\rho = \rho - \rho_0$ where ρ_0 is the residual resistivity, often varies as $\Delta\rho \sim T^m$ with $m < 2$.

It is generally believed that the NFL behavior observed in HFS at the magnetic–nonmagnetic transition arises from a proliferation of low-energy magnetic excitations [3–5]. This transition, being induced by an external parameter such as concentration or pressure, may in principle occur at $T = 0$. If the transition is continuous, it is driven by quantum fluctuations instead of thermal fluctuations in finite-T transitions. The critical behavior of such a Quantum Phase Transition (QPT) at $T = 0$ is governed by the dimension d and the dynamical exponent z. In the Hertz–Millis theory [3,4] the effective dimension is given by $d_{\text{eff}} = d + z$. Hence one is in general above the upper critical dimension $d_{\text{eff}} = 4$ except in the marginal case $d = z = 2$.

While in three spatial dimensions the renormalization-group treatment by Millis [4] essentially corroborates the previous predictions of the Self-Consistent Renormalization (SCR) theory of spin fluctuations [5], new results are obtained for two-dimensional (2D) systems. The case of 2D fluctuations coupled to itinerant quasiparticles with 3D dynamics has been worked out by Rosch *et al.* [6]. This case is pertinent to the unusual situation in $CeCu_{6-x}Au_x$ as will be explained below.

In this review, we will focus on $CeCu_{6-x}Au_x$ which appears to be one of the best studied examples of NFL behavior where macroscopic (thermodynamic and transport properties) as well as microscopic measurements (elastic and inelastic neutron scattering) have been performed. As we will see, this system presents very unusual spin dynamics. In addition, we will discuss how the parameters Au concentration, hydrostatic pressure or magnetic field are operative in tuning the system through a QPT. Again, $CeCu_{6-x}Au_x$ is quite unique in this aspect since all these parameters have been employed early on [7,8].

This paper is organized as follows: Section 2 reviews the salient features of antiferromagnetic order occurring for $x > x_c \approx 0.1$. Section 3 gives an overview over the magnetic fluctuations close to the QPT at x_c determined by inelastic neutron scattering. Section 4 discusses the effect of hydrostatic pressure and magnetic field in the vicinity of a QPT. The conclusions are presented in Section 5. The reader who is interested in more details about $CeCu_{6-x}Au_x$ is referred to a review of macroscopic non-Fermi-liquid properties [9], to a discussion of the interplay of magnetic structure and electronic transport [10], and to a general review of Fermi-liquid instabilities at the magnetic–nonmagnetic transition [11].

2. Antiferromagnetic order of CeCu$_{6-x}$Au$_x$

CeCu$_6$ crystallizes in the orthorhombic Pnma structure and undergoes an orthorhombic-monoclinic phase transition around $T_{om} \approx 220$ K. The monoclinic distortion is only small ($\sim 1.5°$). In order to avoid confusion, we use the orthorhombic notation for the crystallographic directions throughout this paper. T_{om} decreases linearly with increasing x and vanishes at $x \approx 0.14$ [12]. A detailed study of the orthorhombic-monoclinic transition under pressure by means of thermal-expansion measurements has shown that it is not related to the magnetic instability [13]. Pure CeCu$_6$ is a HFS showing no long-range magnetic order down to the range of ~ 20 mK [14, 15]. With $\gamma = 1.6$ J/moleK^2 it is one of the "heaviest" HFS. CeCu$_6$ exhibits a pronounced magnetic anisotropy with the magnetization ratios along the three axes $M_c : M_a : M_b \approx 10 : 2 : 1$ at low T [15].

Several groups have reported evidence for magnetic ordering (either electronic or nuclear) occurring at a few mK [16, 17]. These findings have been substantiated recently with measurements of the magnetic susceptibility χ and thermal expansion [18]. Surprisingly, the observed maximum in $\chi(T)$ found at $T \approx 2$ mK is strongest for magnetic field along the a direction, as opposed to the c direction being the easy direction above ~ 0.1 K. The $\chi(T)$ maximum is suppressed in weak fields of the order of 3 mT, corresponding to the low ordering temperature.

Already at relatively high T, *i.e.* around 1 K, does CeCu$_6$ exhibit intersite antiferromagnetic fluctuations as observed with Inelastic Neutron Scattering (INS) by peaks in the dynamic structure factor $S(\boldsymbol{q}, \omega)$ for energy transfer $\hbar\omega = 0.3$ meV at $\boldsymbol{Q} = (100)$ and $(0\ 1 \pm 0.15\ 0)$ [19, 20]. The rather large widths of these peaks correspond to correlation lengths extending roughly only to the nearest Ce neighbors. Recently, additional features in the a^*c^* plane at an energy transfer of 0.1 meV were found [21]. These correlations vanish in a field of ~ 2 T. The breaking of the antiferromagnetic correlations by a magnetic field (often referred to as metamagnetic transition) has also been observed in the differential magnetic susceptibility dM/dB as a shallow maximum at 2 T at very low T [22].

Upon alloying with Au the CeCu$_6$ lattice expands [23], thus weakening the hybridization between conduction electrons and Ce $4f$ electrons. Hence the conduction-electron$-4f$-electron exchange constant J decreases, leading to a stabilization of localized magnetic moments which can now interact via the RKKY interaction. The result is antiferromagnetic order in CeCu$_{6-x}$Au$_x$ beyond a threshold concentration $x_c \approx 0.1$, as inferred early on from sharp maxima in the specific heat $C(T)$ [24], ac susceptibility [24, 25] and dc magnetization $M(T)$ [24, 26]. For $0.1 < x \leq 1$ the Néel temperature T_N varies linearly with x. For the stoichiometric compound CeCu$_5$Au

where the Au atoms completely and exclusively occupy the Cu(2) site of CeCu$_6$ [27], a complex magnetic phase diagram has been mapped out [28].

The magnetic structure of CeCu$_{6-x}$Au$_x$ $(0.15 \le x \le 1)$ was determined with elastic neutron scattering [10,29,30]. Fig. 1(a) and (b) shows results of elastic scans across magnetic Bragg reflections for $x = 0.15$ and 0.2, taken at temperatures below the ordering temperature $T_N \approx 0.08$ K and ≈ 0.25 K, respectively.

The observed resolution-limited reflections for $x = 0.2$ in the a^*c^* plane (Fig. 1(b)), indicate long-range magnetic order at $\boldsymbol{Q} = (0.625 \; 0 \; 0.275)$. For $x = 0.15$, a somewhat broader Bragg reflection is found (Fig. 1(a)), resulting in the same ordering wave vector $\boldsymbol{Q}$. The larger-than-resolution-limited width may result from the fact that the measuring temperature $(T \approx 50$ mK) was not sufficiently below T_N. Note also the small intensity of the magnetic Bragg reflection. Only minor changes in the positions of the magnetic peaks are found for $x = 0.3$ with $\boldsymbol{Q} = (0.62 \; 0 \; 0.253)$ [10] and $x = 0.4$ where $\boldsymbol{Q} = (0.605 \; 0 \; 0.22)$. [30]. In contrast, upon further Au doping, the magnetic order for $x = 0.5$ no longer appears off the a^* axis, but incommensurate order is observed along a^* with $\boldsymbol{Q} = (0.59 \; 0 \; 0)$ [29] which is then roughly constant up to $x = 1$ $(\boldsymbol{Q} = (0.56 \; 0 \; 0))$. Assuming a sinusoidal modulation of the moments aligned along c we estimate an average ordered magnetic moment μ of 0.1 to 0.15 μ_B/Ce atom for $x = 0.2$. Under the same assumptions the ordered moment for $x = 0.3$ is a factor of 3 larger [10]. For $x = 0.5$, $\mu \approx 1 \mu_B$/Ce atom is estimated [29]. μ increases only by small percentage for $x = 1$. Theoretically [5], the ordered magnetic moment in a weakly interacting itinerant-electron model should depend on the Néel temperature as $\mu \propto T_N^{3/4}$ which is quite different from $\mu(T_N)$ experimentally observed. The possible differences of the magnetic structure for $x = 0.5$ and 1 are discussed elsewhere [10].

For $x = 0.2$ we find short-range magnetic order along the a^* axis with a wave vector $\boldsymbol{\tau} = (0.79 \; 0 \; 0)$ in addition to the long-range order mentioned above.

From the linewidth of the peaks, $\Delta q = 0.06$ r.l.u. (HWHM) in a^*, we deduce a correlation length of about 2.7 unit cells in the a direction which is somewhat smaller than the result previously reported [6] (there a factor of $1/2\pi$ was omitted).

Fig. 2 shows $\rho(T)$ for different CeCu$_{6-x}$Au$_x$ alloys for current parallel to the orthorhombic a direction. For $x < x_c \approx 0.1$, $\rho(T)$ increases at the lowest temperatures as $\rho(T) = \rho_0 + AT^2$ which is expected for a FL with dominant quasiparticle-quasiparticle scattering for $T \to 0$ as has been observed before for CeCu$_6$ [15]. For the magnetically ordered alloys with $0.15 \le x \le 0.3$, $\rho_a(T)$ and $\rho_c(T)$ (not shown) exhibit a kink a T_N and increase with decreasing $T < T_N$. These findings can be qualitatively interpreted in terms of
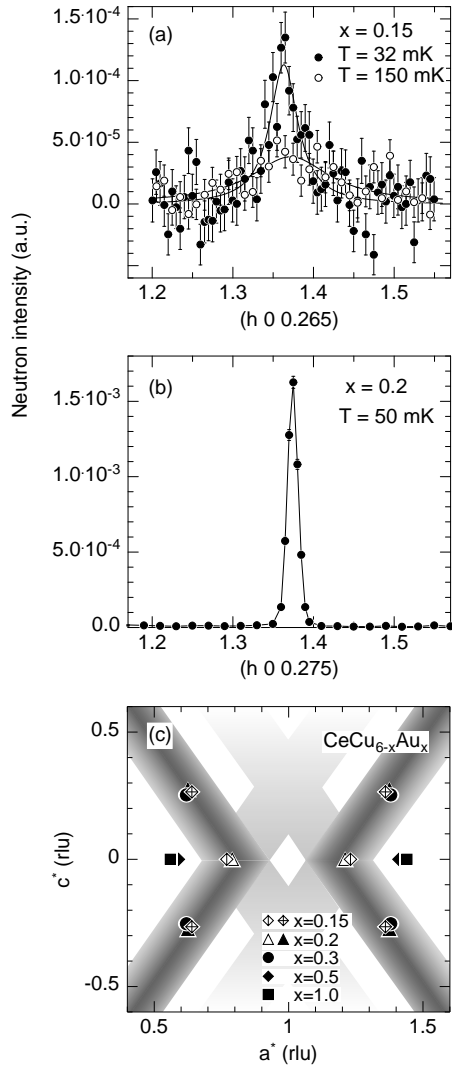
Fig. 1. (a) Neutron scattering intensity for elastic scans of $CeCu_{5.85}Au_{0.15}$ along $(h\,0\,0.265)$ as measured on IN 14 with incident neutron energy of $E_0 = 3.24\,\mathrm{meV}$ below and above $T_N = 80\,\mathrm{mK}$. (b) Scan of $CeCu_{5.8}Au_{0.2}$ along $(h\,0\,0.275)$ measured on IN 14 with $E_0 = 2.74\,\mathrm{meV}$ below $T_N = 0.25\,\mathrm{K}$. (c) Position of the magnetic Bragg peaks for $0.15 \leq x \leq 1$ in the reciprocal ac plane of $CeCu_{6-x}Au_x$. Open symbols indicate short-range order peaks with widths larger than the q resolution of the instruments. Shaded strips indicate the dynamic correlations found for $x = 0.1$ (full width half maximum).

the observed magnetic order, $\rho(T)$ increases below T_N for current directions with a non-zero projection of the magnetic ordering vector $\boldsymbol{Q}$ determined from the elastic neutron-scattering data discussed above [10]. An increase of $\rho(T)$ below T_N has been observed before in other HFS, for example, in $Ce_{1-x}La_xRu_2Si_2$ [31] and $CeRu_{2-x}Rh_xSi_2$ [32]. For $x = 0.10$ where $T_N \to 0$, the T-dependent part of the resistivity $\Delta\rho$ increases quasilinearly with T, signaling NFL behavior.
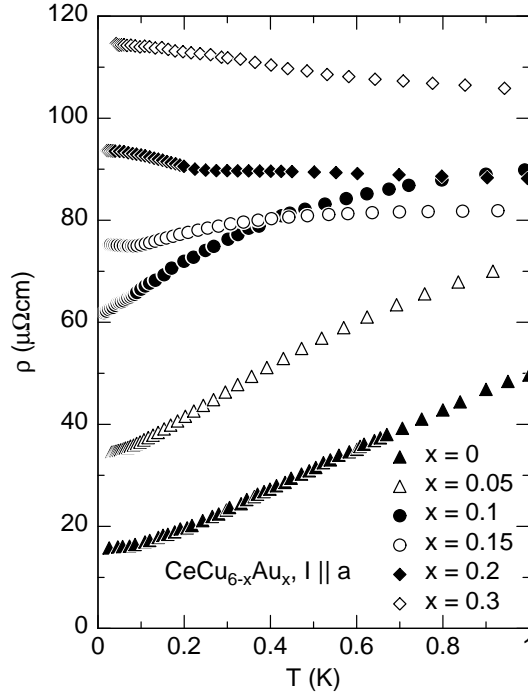

Fig. 2. Electrical resistivity $\rho(T)$ of $CeCu_{6-x}Au_x$ $(0 \leq x \leq 0.3)$ for current along the a direction.

3. Magnetic fluctuations near the quantum critical point

For $CeCu_{6-x}Au_x$, near the critical concentration $x = 0.1$ for the onset of magnetic order, an unusual T dependence of thermodynamic and magnetic properties has been observed in addition to the T-linear resistivity mentioned above [7]. The linear specific-heat coefficient depends logarithmically on T, $C/T = a\ln(T_0/T)$, between 0.06 and 2.5 K, with $a = 0.58\,\mathrm{J/molK^2}$ and $T_0 = 6.2\,\mathrm{K}$, the latter corresponding to the Kondo temperature T_K of pure $CeCu_6$ [15]. The magnetic susceptibility was found to vary as $\chi \approx M/B \sim 1 - a'\sqrt{T}$ between 0.08 and 3 K where M is the dc magnetization measured in

a magnetic field $B \approx 0.1\,\mathrm{T}$ [7]. Motivated by INS data (see below), Schröder *et al.* showed that the $\chi(T)$ data can be described very well by a different functional dependence, *i.e.* $\chi(T)^{-1} - \chi(0)^{-1} = a''T^{\alpha}$ with $\alpha = 0.8$ [33]. This fit extends to $7\,\mathrm{K}$, *i.e.* to well above T_{K}. This is surprising because the FL regime in pure $CeCu_6$ is observed only well below T_{K}.

The abundance of low-energy magnetic excitations when T_{N} is just tuned to zero, has been suggested early on to cause the NFL behavior at the magnetic instability [7]. However, the $-\ln T$ dependence of C/T and the linear T dependence of ρ in $CeCu_{6-x}Au_x$ at the magnetic instability have constituted a major puzzle ever since they were first reported, because spin-fluctuation theories for 3D itinerant fermion systems predict [4,5] $C/T = \gamma_0 - \beta\sqrt{T}$ and $\Delta\rho \sim T^{3/2}$ for antiferromagnets ($z = 2$) in the limit $T \to 0$). In addition, T_{N} should depend on the control parameter $\delta_x = x - x_{\mathrm{c}}$ or $\delta_p = p - p_{\mathrm{c}}$ as $T \sim \mid \delta \mid^{\zeta}$ with $\zeta = z/(d + z - 2) = z/(z + 1)$ for $d = 3$ [4], while for $CeCu_{6-x}Au_x$ $\zeta \approx 1$ for both δ_x [7] and δ_p [8] is found. In order to resolve this puzzle, a search for critical fluctuations by INS was performed. The short-range magnetic ordering found for $x = 0.2$ along the a^* axis [34] prompted Rosch *et al.* [6] to suggest an effectively 2D magnetic ordering on the basis that the broad feature observed along a^* exhibits a much smaller width along b^*. 2D critical fluctuations coupled to quasiparticles with 3D dynamics do indeed lead to the observed behavior $C/T \sim -\ln T$, $\Delta\rho \sim T$ and $T_{\mathrm{N}} \sim \mid \delta \mid$, *i.e.* $\zeta = 1$ [6].

A detailed investigation at the critical concentration $x = 0.1$ by Stockert *et al.* [35] showed that, as a matter of fact, the critical fluctuations as measured with an energy transfer of $0.10\,\mathrm{meV}$ are not confined to the a^* axis but extend into the a^*c^* plane. This is inferred from a large number of scans in the a^*c^* plane, some of which are shown in Fig. 3. Here the dynamical structure factor $S(\boldsymbol{q}, \hbar\omega = 0.10\,\mathrm{meV})$ has the form of rods as indicated by the shaded regions in Fig. 1(c). Yet, the main conclusion of earlier work [6] remains valid, namely the presence of a quasi-1D dynamic feature in reciprocal space that corresponds to quasi-2D fluctuations in real space. The width of $S(\boldsymbol{q}, \hbar\omega)$ perpendicular to the rods is roughly a factor of five smaller than along the rods. This is found for scans within the a^*c^* plane and also perpendicular to the a^*c^* plane, *i.e.* in the b^* direction [35]. The 3D ordering peaks for $x = 0.15, 0.2$ and 0.3 fall on the rods for $x = 0.1$ which therefore can be viewed as precursors of 3D ordering.

From the width of the rods in reciprocal space, the prefactor a of the logarithmic C/T dependence could be calculated to within a factor of two of the experimental value [35].

The spin fluctuations also develop specific dynamics at $x = 0.1$ [33]. The scattering function $S(\boldsymbol{q}, E, T)$ or the susceptibility $\chi'' = S(1 - \exp(-E/k_{\mathrm{B}}T))$ exhibit E/T scaling ($E = \hbar\omega$) in the critical $\boldsymbol{q}$ region, *e.g.* at $\boldsymbol{Q}_{\mathrm{c}} = (0.8\,0\,0)$,
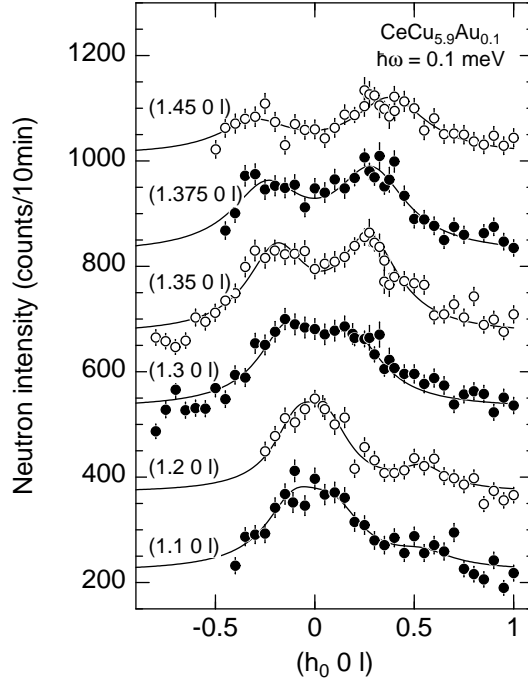
Fig. 3. Neutron scattering intensity of $CeCu_{5.9}Au_{0.1}$ for scans along $(h_0\ 0\ l)$ for various fixed $h_0 = 1.1 \dots 1.45$ with neutron energy transfer $\hbar\omega = 0.1\,\mathrm{meV}$ and fixed final energy $E_\mathrm{f} = 2.74\,\mathrm{meV}$ at $T = 70\,\mathrm{mK}$. The scans are shifted by 150 counts with respect to each other.

which can be expressed by

$$\chi''(\boldsymbol{Q}_\mathrm{c}, E, T) = T^{-\alpha}g(E/k_\mathrm{B}T) \tag{1}$$

with $\alpha = 0.75$ [33], see Fig. 4. This demonstrates that the characteristic energy scale of the correlated fluctuations at this QPT is nothing else but $k_\mathrm{B}T$. The exponent $\alpha \neq 1$ indicates that the fluctuations do not have a Lorentzian lineshape. These data have been supplemented recently by data taken at various $\boldsymbol{q}$. It was found that the anomalous non-Lorentzian response does not change for other $\boldsymbol{q}$ away from the critical region [38]. For all $\boldsymbol{q}$, the susceptibility can be expressed as

$$\chi^{-1}(\boldsymbol{q}, E, T) = c^{-1}\left(f(\boldsymbol{q}) + (-iE + aT)^\alpha\right). \tag{2}$$

In particular, the T dependence of the static uniform susceptibility $\chi(\boldsymbol{q} = 0, E = 0) \approx M/B$ can be described by

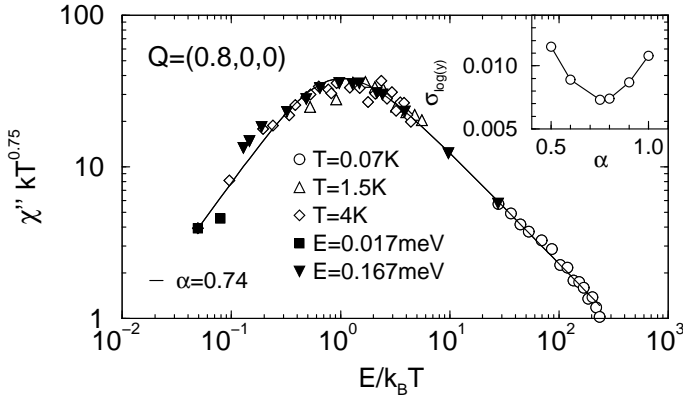$$\chi^{-1}(T) - \chi^{-1}(0) = c^{-1}aT^\alpha \tag{3}$$

Fig. 4. Scaling plot of inelastic neutron scattering data at $Q = (0.8\ 0\ 0)$ for $CeCu_{5.9}Au_{0.1}$ *vs* $E/k_B T$ where E is the neutron energy transfer. Solid line corresponds to a fit derived from Eq. (2) with $\alpha = 0.74$ and $f(q) = 0$. The inset shows deviations from the mean value per interval of $E/k_B T$ to check the quality of the scaling collapse with varying α.

with the same exponent $\alpha \approx 0.8$ to a high degree of accuracy, as mentioned above. The simple form of Eq. (2) separates static spatial correlations from the specific temporal correlations, the latter being independent of q. These local fluctuations at the quantum critical point show a significant departure from FL behavior since $\alpha < 1$. Putting this scenario into a QPT framework with the only parameters d and z, consistency with the specific heat C can be shown by modeling $f(q)$ with a q^2 dependence perpendicular to the rod structure and by a vanishing q^2 term but a finite q^4 term parallel to the rods. This leads to $z = 2.5$ and $d_{\text{eff}} = 2.5$, thus obeying the condition $d = z$ for a vanishing power in C/T, consistent with a logarithmic T dependence [33]. The scenario of a locally critical quantum phase transition has received considerable theoretical attention, although a detailed model is not available yet [36, 37]. As a possible test, measurements of the Hall coefficient around the quantum critical point have been suggested [37]. We wish to point out that the evolution of the ordered moment with increasing $x > x_c$ discussed above, may provide a valuable input to test the different models.

While the two neutron-scattering data sets for $x = 0.1$ [33, 35] are not contradictory, the two interpretations lead to different predictions, depending on how the T dependence of the weakly correlated fluctuations along the rod direction is treated. The difference between absence or presence of a weak T dependence, yielding $d = 2$ or $d_{\text{eff}} = 2.5$ respectively, cannot be distinguished by the present data sets. However, one essential common ingredient in both models is the unusual low effective dimension for the critical

fluctuations in this material. A further point is that it is not easy to see where an effective 2D fluctuation spectrum originates from. The 2D planes are spanned by the b axis and the connecting line between next-nearest-neighbor Ce atoms. Only a microscopic model can establish if, perhaps, the low dimensionality arises from a strong anisotropy of the Fermi surface, the RKKY interaction, conduction-electron−local-moment hybridization, or a combination of these effects. On the other hand, the low dimensionality might turn out to be a more generic characteristic of a QPT in HFS.

Despite these open questions it should be stressed that $CeCu_{6-x}Au_x$ is one of the best characterized HFS exhibiting NFL behavior. It is rewarding that the unusual behavior of the thermodynamic and transport properties at the QPT can be traced back to an unusual low-dimensional fluctuation spectrum determined by inelastic neutron scattering.

The unusual q dependence of the fluctuations exists even away from the QPT. Fig. 5 shows scans for $x = 0.2$ in the a^*c^* plane taken at $50\,mK$ with an energy transfer $\hbar\omega = 0.15\,meV$. Overall similar features to those
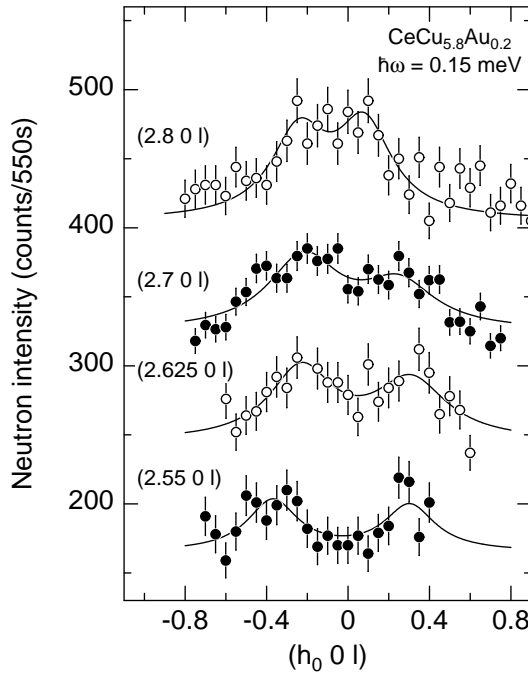

Fig. 5. Neutron scattering intensity of $CeCu_{5.8}Au_{0.2}$ for scans along $(h_0\ 0\ l)$ for fixed $h_0 = 2.55, 2.625, 2.7$ and 2.8 with neutron energy transfer $\hbar\omega = 0.15\,meV$ and $E_f = 2.74\,meV$ at $T = 50\,mK$. The scans are shifted by 80 counts with respect to each other.

for $x = 0.1$ are found for this magnetically ordered alloy ($T_N \approx 0.25\,\mathrm{K}$). These rod-like dynamic correlations coexist with the 3D long-range ordering at $\boldsymbol{Q} = (0.625\ 0\ 0.275)$ observed below T_N and the short-range order at $\boldsymbol{\tau} = (0.8\ 0\ 0)$ observed below $\sim 0.5\,\mathrm{K}$. In fact, the dynamic correlations persist up to much higher T, *i.e.*, up to several K, similar to what is observed for $x = 0.1$ [33, 35]. Fig. 6 shows that the correlations at $T = 0.3\,\mathrm{K}$, *i.e.*, above T_N have not lost intensity by any appreciable amount with respect to $T < T_N$.
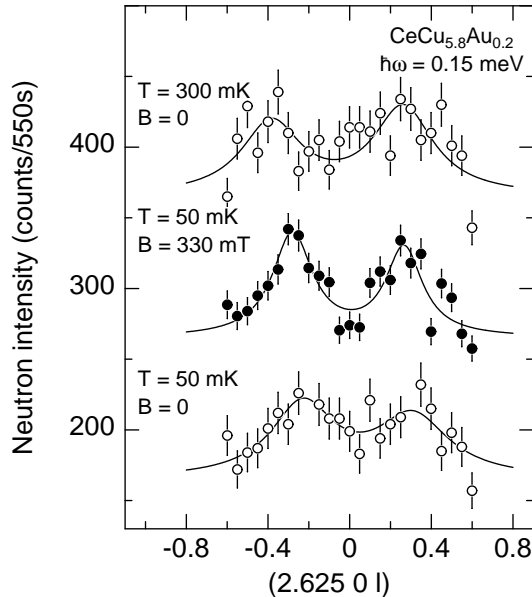

Fig. 6. Neutron scattering intensity of $CeCu_{5.8}Au_{0.2}$ for scans along $(2.625\ 0\ l)$, $\hbar\omega = 0.15\,\mathrm{meV}$, $E_f = 2.74\,\mathrm{meV}$ at temperatures $T = 50\,\mathrm{mK}$ below T_N for magnetic field $B = 0$ and $0.33\,\mathrm{T}$, and at $T = 300\,\mathrm{mK}$ above T_N for $B = 0$. The scans are shifted by 100 counts with respect to each other.

4. Effect of pressure and magnetic field in the vicinity of the quantum critical point

The onset of magnetic order in the $CeCu_{6-x}Au_x$ system is attributed to a weakening of J because of the increase of the molar volume upon alloying with Au. Indeed, T_N of $CeCu_{6-x}Au_x$ decreases roughly linearly under hydrostatic pressure p [8,39]. Although the volume effect is dominant in the competition between magnetic and nonmagnetic groundstates in $CeCu_{6-x}Au_x$, other effects also play a role, notably the anisotropic compressibility [13] and the anisotropic change of the lattice constants upon Au doping (a and c
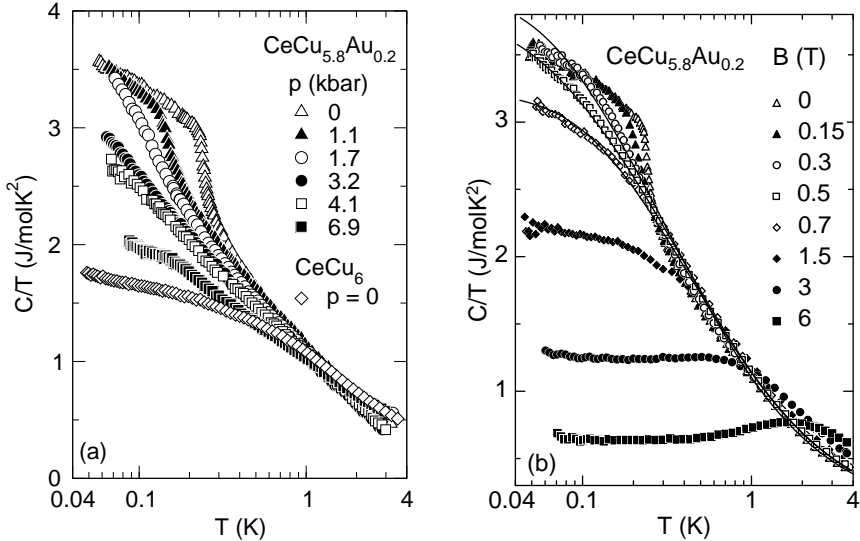
Fig. 7. (a) Specific heat C of $CeCu_{5.8}Au_{0.2}$ for different hydrostatic pressures p, plotted as C/T *vs* T on a logarithmic scale. Also shown are the data for $CeCu_6$ at ambient pressure. (b) C/T *vs* T on a logarithmic scale of $CeCu_{5.8}Au_{0.2}$ for different applied magnetic fields B. Solid lines indicate fits of the Moriya–Takimoto model of spin fluctuations to the data for $B = 0.3, 0.5$ and 0.7 T. See text for details.

expand while b contracts up to $x = 1$) [23]. Furthermore, the anisotropic dependence of T_N on uniaxial stress σ is striking: While T_N decreases for $\sigma \parallel b$ and $\sigma \parallel c$, it increases for $\sigma \parallel a$ [40,41]. Under hydrostatic pressure, $T_N \approx 0$ is reached at 7–8 kbar for $x = 0.3$ [8], and at 3.2–4 kbar for 0.2 [40]. At these hydrostatic pressures both alloys exhibit NFL behavior in the specific heat, *i.e.*, $C/T \sim -\ln T$, with, surprisingly, the same coefficients a and T_0 for both, and additionally for the NFL alloy with $x = 0.1$ and at $p = 0$. Specific-heat data for $x = 0.2$, plotted as C/T *vs* $\ln T$, are shown in Fig. 7(a) for various hydrostatic pressures. On the other hand, application of pressure for $x = 0.1$ drives this alloy towards FL behavior: for $p = 6.0$ kbar, C/T falls even below the data of pure $CeCu_6$ at $p = 0$ [11]. This shows how nicely both composition and pressure can be employed to tune the QPT.

One might ask whether NFL behavior may arise at a magnetic-field induced instability in magnetically ordered $CeCu_{6-x}Au_x$ for $x > 0.1$. In the light of the preceding discussion, however, it would be astonishing if an applied magnetic field along the easy c direction would induce low-lying 2D spin excitations. An apparent inducement of NFL behavior in a polycrystalline $CeCu_{4.8}Ag_{1.2}$ alloy by a magnetic field was reported previously by Heuser *et al.*, *i.e.*, approximately $C/T \sim -\ln(T/T_0)$ between 0.35 and 2.5 K [42].

Subsequently, the same group reported specific-heat data down to 0.07 K on a CeCu$_{5.2}$Ag$_{0.8}$ single crystal with $T_N = 0.7$ K [44]. At a critical magnetic field $B_c = 2.3$ T applied to the easy direction, C/T varies logarithmically between ~ 1.5 and 0.2 K and then levels off towards lower T, in line with a $\gamma_0 - \beta\sqrt{T}$ dependence. Moreover, the resistivity exhibits a $T^{1.5}$ dependence at B_c. Thus the data appear to be compatible with the conventional spin-fluctuation scenario, with $d = 3$ and $z = 2$.

Elastic neutron-scattering measurements of the (2.625 0 0.275) reflection for CeCu$_{5.8}$Au$_{0.2}$ with $B \parallel c$ show that its intensity decreases linearly with B and vanishes around $B_c \approx 0.42$ T for $T = 50$ mK [43]. Fig. 7(b) shows the specific heat of this sample for various applied magnetic fields B. Again, T_N is suppressed with increasing B. For fields just below and above B_c, *i.e.*, $B = 0.3$ T and 0.5 T, we observe a negative curvature in C/T *vs* $\ln T$ towards low T, distinctly different from the T dependence observed in pressure tuning the QPT. Here we have subtracted the hyperfine contribution $C_{hf} = b_N T^{-2}$ due to the Zeeman splitting of ^{63}Cu and ^{65}Cu nuclei. The specific-heat data at $B = 0.3$ and 0.5 T may be modeled quite accurately by the self-consistent 3D spin-fluctuation model as given by Moriya and Takimoto [5], assuming that this model is appropriate at comparatively small fields.

By using the full finite-T expression for the specific heat C, Eq. (4.5) of Ref. [5], we obtain a good fit for $B = 0.5$ T with the parameters $y_0 = 0.01$, $y_1 = 8$, and $T_A = 2.8$ K (solid line in Fig. 7(b)). This expression yields a low-T asymptotic dependence $C/T = \gamma_0 - \beta T^{0.5}$ previously observed for CeCu$_{6-x}$Ag$_x$. Even the data for $B = 0.7$ T, may be fitted very well by $y_0 = 0.032$, an unchanged y_1, and a slightly changed $T_A = 2.9$ K. It is remarkable that the agreement reaches as high as 4 K, although the range of validity, in principle, is constrained to temperatures well below the Kondo temperature. However, only a model going beyond the various approximations employed here, addressing the field dependence over a large range, is expected to show if the behavior near B_c may indeed be interpreted as a field-induced *quantum* phase transition.

We now turn to the electrical resistivity $\rho(T)$ for $x = 0.2$ for several hydrostatic pressures p, measured with the electrical current along the a direction, see Fig. 8(a). The decrease of T_N with increasing p is directly visible in $\rho(T)$, with T_N vanishing around ≈ 5 kbar, in reasonable agreement with the specific-heat results. We can extract a linear T dependence of $\rho(T)$ over a limited T range above 5 kbar. The quasi-linear T dependence of $\rho(T)$ for $p = 7$ kbar resembles that of $\rho(T)$ for $x = 0.1$ at $p = 0$.

The effect of a magnetic field on $\rho(T)$ and on ρ_0 is rather small compared to that of p (Fig. 8(b)). Furthermore, the best fit for $\rho(T) = \rho_0 + A''T^m$ at $B = 0.4$T $\approx B_c$ (solid line in Fig. 8c) yields $m = 1.48 \pm 0.03$, again in very good agreement with the 3D spin-fluctuation scenario. For $B = 0.7$ T, a $T^{1.5}$
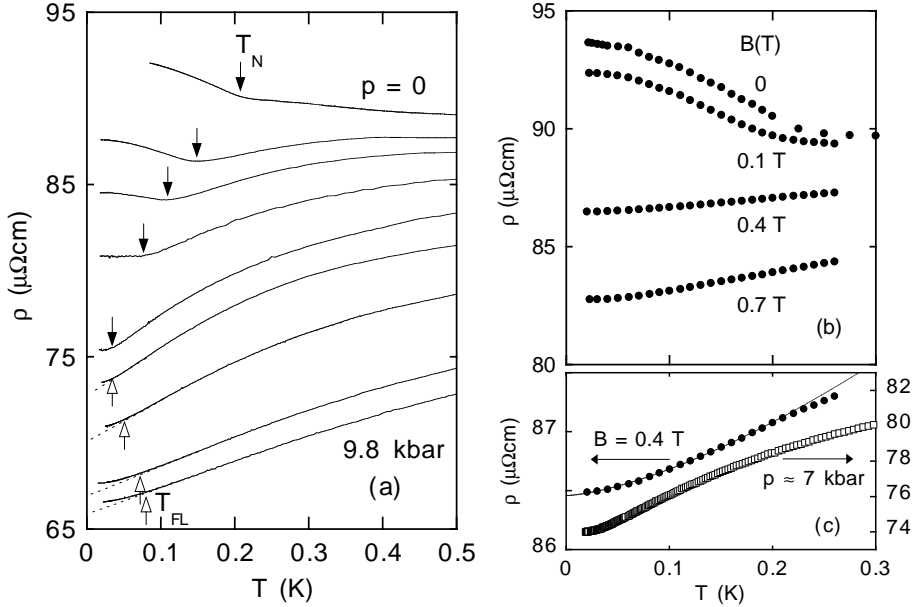
Fig. 8. (a) Electrical resistivity ρ vs temperature T of CeCu$_{5.8}$Au$_{0.2}$ for various hydrostatic pressures $p = 0$, 1.3, 2.4, 3.5, 4.1, 7.0, 8.1, 9.3, and 9.8 kbar (from top to bottom). Solid arrows indicate the Néel temperature T_N, open arrows the crossover temperature T_{FL} below which ρ exhibits a T^2 dependence. (b) ρ vs T of CeCu$_{5.8}$Au$_{0.2}$ for various magnetic fields B. (c) Comparison of the T dependence of ρ near the magnetic-nonmagnetic transition obtained by field tuning ($B = 0.4$ T) and pressure tuning ($p = 7$ kbar).

fit still is satisfactory, although the data at low T are better described by a T^2 behavior. The clear distinction of the resistivity $\rho(T)$ for pressure tuning vs. field tuning the QPT, *i.e.* for p_c and B_c, is emphasized in Fig. 8(c) where the different T dependencies of $\rho(T)$ are clearly visible.

The different behavior of $C(T)$ and $\rho(T)$ at the QPT tuned by B or p presents strong evidence for pronounced differences in the fluctuation spectra. The pressure-tuning results suggest that the strongly anisotropic fluctuation spectrum observed for $x = 0.1$ at ambient pressure which can be modeled by quasi-2D fluctuations, prevails. One may expect that likewise the unexpected energy–temperature scaling of the dynamic susceptibility $\chi^{-1}(q, E) = c^{-1}(f(q) + (-iE + aT)^{\alpha})$ with $\alpha = 0.75$ observed for $x = 0.1$ at $p = 0$ [38], survives at the QPT under pressure.

On the other hand, a magnetic field appears to drive the system towards a more isotropic 3D fluctuation spectrum. Inelastic neutron scattering studies under pressure and in a magnetic field as well as further uniaxial-

stress studies are necessary in order to qualify the findings of the present study and to establish a possible link to the field–temperature scaling of the uniform static susceptibility found recently for $CeCu_{5.9}Au_{0.1}$ [38]. It will be interesting to compare the magnetic order and spin dynamics in $CeCu_{6-x}Ag_x$ and $CeCu_{6-x}Au_x$ in a magnetic field. A preliminary measurement for $CeCu_{5.8}Au_{0.2}$ (Fig. 6) shows that the fluctuations prevail in a magnetic field $B = 0.33\,T$, *i.e.* close to B_c.

5. Conclusions

$CeCu_{6-x}Au_x$ is one of the best characterized systems displaying the competition between Kondo effect leading to local singlets and RKKY interaction leading to long-range magnetic order. The incommensurate antiferromagnetic order observed for $x > 0.1$ has been investigated in detail by elastic neutron scattering. An unexpected feature is the jump of the magnetic ordering vector occurring between $x = 0.3$ and 0.5. The anomalous behavior of the thermodynamic and transport properties of $CeCu_{6-x}Au_x$ at the quantum critical point $x_c \approx 0.1$ between nonmagnetic and magnetically ordered groundstates is attributed to magnetic fluctuations with an effective dimension smaller than three. While the dynamic fluctuations measured at fixed energy transfer have a pronounced $\boldsymbol{q}$ dependence with a strong anisotropy, unexpected for a precursor of three-dimensional magnetic ordering, the dynamic susceptibility is determined by unusual temporal correlations that are independent of $\boldsymbol{q}$, *i.e.* local in character. This sheds new light on the interplay between long-range magnetic correlations and local dynamics at the quantum critical point. Recently, the $YbRh_2(Si_{1-x}Ge_x)_2$ system where magnetic order found for $x = 0$ is suppressed by expansion of the lattice via Ge doping [45], has been shown [46] to exhibit similar field–temperature scaling of the uniform static susceptibility as $CeCu_{5.9}Au_{0.1}$. While concentration and hydrostatic pressure can be employed for $CeCu_{6-x}Au_x$ as parameters to tune the quantum critical point in a qualitatively similar fashion, magnetic field acts differently. Overall, field has a similar influence as temperature in driving the system away from a quantum critical point. For magnetically ordered alloys with $x > 0.1$, field may induce a magnetic–nonmagnetic transition with a behavior reminiscent of 3D antiferromagnetic spin fluctuations. Detailed neutron scattering studies have to be performed in order to check this scenario and to search for quantum critical fluctuations.

REFERENCES

[1] S. Doniach, *Physica B* **91**, 213 (1977).

[2] See, *e.g.*: Proceedings of the Conference on Non-Fermi-Liquid Behavior on Metals, Santa Barbara 1996, published as special issue of *J. Phys.: Condens. Matter.* **8**, (1996).

[3] J.A. Hertz, *Phys. Rev.* **B14**, 1165 (1976).

[4] A.J. Millis, *Phys. Rev.* **B48**, 7293 (1993).

[5] T. Moriya, T. Takimoto, *J. Phys. Soc. Jpn.* **64**, 960 (1995), and references therein.

[6] A. Rosch, A. Schröder, O. Stockert, H. v. Löhneysen, *Phys. Rev. Lett.* **79**, 150 (1997).

[7] H. v. Löhneysen, T. Pietrus, G. Portisch, H.G. Schlager, A. Schröder, M. Sieck, T. Trappmann, *Phys. Rev. Lett.* **72**, 3262 (1994).

[8] B. Bogenberger, H. v. Löhneysen, *Phys. Rev. Lett.* **74**, 1016 (1995).

[9] H. v. Löhneysen, *J. Phys.: Condens. Matter.* **8**, 9689 (1996).

[10] H. v. Löhneysen, A. Neubert, T. Pietrus, A. Schröder, O. Stockert, U. Tutsch, M. Loewenhaupt, A. Rosch, P. Wölfle, *Eur. Phys. J.* **B5**, 447 (1998), and references therein.

[11] H. v. Löhneysen, *J. Magn. Magn. Mater.* **200**, 532 (1999).

[12] H. v. Löhneysen, A. Schröder, O. Stockert, *J. Alloy. Compd.* **303-304**, 480 (2000).

[13] K. Grube, W. H. Fietz, U. Tutsch, O. Stockert, H. v. Löhneysen, *Phys. Rev.* **B60**, 11947 (1999).

[14] Y. Onuki, T. Komatsubara, *J. Magn. Magn. Mater.* **63 & 64**, 281 (1987).

[15] A. Amato, D. Jaccard, J. Flouquet, F. Lapierre, J.L. Tholence, R.A. Fisher, S.E. Lacy, J.A. Olson, N.E. Phillips, *J. Low Temp. Phys.* **68**, 371 (1987).

[16] E. A. Schuberth, J. Schupp, R. Freese, K. Andres, *Phys. Rev.* **B51**, 12892 (1995).

[17] L. Pollack, M.J.R. Hoch, C. Jin, E.N. Smith, J.M. Parpia, D.L. Hawthorne, D.A. Geller, D.M. Lee, R.C. Richardson, D.G. Hinks, E. Bucher, *Phys. Rev.* **B52**, R15707 (1995).

[18] H. Tsujii, E. Tanaka, Y. Ode, T. Katoh, T. Mamiya, S. Araki, R. Settai, Y. Ōnuki, *Phys. Rev. Lett.* **84**, 5407 (2000).

[19] G. Aeppli, H. Yoshizawa, Y. Endoh, E. Bucher, J. Hufnagl, Y. Ōnuki, T. Komatsubara, *Phys. Rev. Lett.* **57**, 122 (1986).

[20] J. Rossat-Mignod, L.P. Regnault, J.L. Jacoud, C. Vettier, P. Lejay, J. Flouquet, E. Walker, D. Jaccard, A. Amato, *J. Magn. Magn. Mat.* **76 & 77**, 376 (1988).

[21] O. Stockert *et al.*, to be published.

[22] H. v. Löhneysen, H.G. Schlager, A. Schröder, *Physica B* **186-188**, 590 (1993).

[23] T. Pietrus, B. Bogenberger, S. Mock, M. Sieck, H. v. Löhneysen, *Physica B* **206 & 207**, 317 (1995).

[24] A. Germann, A.K. Nigam, J. Dutzi, A. Schröder, H. v. Löhneysen, *J. Physique Coll.* **49**, C8-755 (1988).

[25] M.R. Lees, B.R. Coles, *J. Magn. Magn. Mater.* **76 & 77**, 173 (1988).

[26] H.G. Schlager, A. Schröder, M. Welsch, H. v. Löhneysen, *J. Low Temp. Phys.* **90**, 181 (1993).

[27] M. Ruck, G. Portisch, H.G. Schlager, M. Sieck, H. v. Löhneysen, *Acta Crystallogr. Sect. B* **49**, 936 (1993).

[28] C. Paschke, C. Speck, G. Portisch, H. v. Löhneysen, *J. Low Temp. Phys.* **97**, 229 (1994).

[29] A. Schröder, J.W. Lynn, R.W. Erwin, M. Loewenhaupt, H. v. Löhneysen, *Physica B* **199 & 200**, 47 (1994).

[30] H. Okumura, K. Kakurai, Y. Yoshida, Y. Ōnuki, Y. Endoh, *J. Magn. Magn. Mater.* **177-181**, 405 (1998).

[31] R. Djerbi, P. Haen, F. Lapierre, P. Lehmann, J.P. Kappler, *J. Magn. Magn. Mater.* **76 & 77**, 260 (1988).

[32] Y. Miyako, S. Kawarazaki, T. Taniguchi, T. Takeuchi, K. Marumoto, R. Hamada, Y. Yamamoto, M. Sato, Y. Tabata, H. Tanabe, M. Ocio, P. Pari, J. Hammann, *Physica B* **230-232**, 1011 (1997).

[33] A. Schröder, G. Aeppli, E. Bucher, R. Ramazashvili, P. Coleman, *Phys. Rev. Lett.* **80**, 5623 (1998).

[34] O. Stockert, H. v. Löhneysen, A. Schröder, M. Loewenhaupt, N. Pyka, P.L. Gammel, U. Yaron, *Physica B* **230-232**, 247 (1997).

[35] O. Stockert, H. v. Löhneysen, A. Rosch, N. Pyka, M. Loewenhaupt, *Phys. Rev. Lett.* **80**, 5627 (1998).

[36] Q. Si, S. Rabello, K. Ingersent, J.L. Smith, cond-mat 0011477 (2000).

[37] P. Coleman, C. Pépin, Q. Si, R. Ramazashvili, *J. Phys. Condens. Matter* **13**, 723 (2001).

[38] A. Schröder, G. Aeppli, R. Coldea, M. Adams, O. Stockert, H. v. Löhneysen, E. Bucher, R. Ramazashvili, P. Coleman, *Nature* **407**, 351 (2000).

[39] A. Germann, H. v. Löhneysen, *Europhys. Lett.* **9**, 367 (1989).

[40] M. Sieck, F. Huster, H. v. Löhneysen, *Physica B* **230-232**, 583 (1997).

[41] F. Obermair, C. Pfleiderer, O. Stockert, H. v. Löhneysen, *Physica B*, in print.

[42] K. Heuser, E.-W. Scheidt, T. Schreiner, G.R. Stewart, *Phys. Rev.* **B57**, R4198 (1998).

[43] H. v. Löhneysen, C. Pfleiderer, T. Pietrus, O. Stockert, B. Will, *Phys. Rev.* **B63**, 134411 (2001).

[44] K. Heuser, E.-W. Scheidt, T. Schreiner, G.R. Stewart, *Phys. Rev.* **B58**, R15959 (1998).

[45] O. Trovarelli, G. Geibel, S. Mederle, C. Langhammer, F.M. Grosche, P. Gegenwart, M. Lang, G. Sparn, F. Steglich, *Phys. Rev. Lett.* **85**, 626 (2000).

[46] O. Trovarelli, F. Steglich, private communication.